Dalton Transactions

ROYAL SOCIETY OF CHEMISTRY

PAPER

View Article Online
View Journal | View Issue

Cite this: *Dalton Trans.*, 2026, **55**, 5224

A systematic series of BODIPY–cyclotriphosphazene conjugates: exploring the effect of BODIPY numbers on photophysical properties

Yacinthe Mariole Mache,[a] Semiha Yıldırım Sarıkaya *[a] and Husniye Ardic Alidagi[b]

Received 7th January 2026,
Accepted 2nd March 2026

DOI: 10.1039/d6dt00037a

rsc.li/dalton

BODIPY dyes (4,4-difluoro-4-bora-3a,4a-diaza-*s*-indacene) have attracted increasing interest for their wide range of potential applications. Herein, a series of BODIPY–cyclotriphosphazene conjugates were synthesized *via* nucleophilic substitution reactions of cyclotriphosphazene with different numbers of distyryl-BODIPY compounds whose conjugation was enhanced by Knoevenagel reaction. Inspired by the enhanced photophysical properties of BODIPY–cyclotriphosphazene compounds reported in the literature compared to those of single BODIPY, we established a strategy to investigate their photophysical properties systematically. The photophysical properties of novel BODIPY–cyclotriphosphazene conjugates (**6–8**) were investigated by UV–Vis and fluorescence spectroscopy in different solvents and at different concentrations, and the results were compared within the series. The obtained findings confirm that, under identical analytical conditions, a consistent bathochromic shift in both absorption and fluorescence spectra occurs with an increasing number of BODIPY units attached to the cyclotriphosphazene core. Additionally, the molar absorptivity of novel cyclotriphosphazenes substituted with two, four and six BODIPY moieties was increased by 1.1-, 1.5- and 3.1-fold, respectively, relative to their precursor BODIPY.

1. Introduction

It is evident that, the past 25 years have witnessed a significant rise in the use of fluorescence across a broad range of modern research applications.[1–3] Small molecular compounds such as BODIPY,[4–6] cyanine,[7] rhodamine,[8] diketopyrrolopyrroles,[9,10] coumarin,[11] fluorescein,[12] quinoline,[13] pyrene,[14] porphyrin[15] and squarine dyes[5] are commonly used in fluorescence-based studies due to their easy and simple synthetic route.[16,17]

Within the wide array of fluorescent molecules, BODIPY derivatives distinguish themselves as one of the most widely employed scaffolds owing to their high fluorescence quantum yields, excellent photophysical stability, and the adjustability of their photophysical properties by the addition of different units to their structures.[5,6,18] Interest in BODIPY dyes, especially near-infrared (NIR)-fluorescence ones (NIR; 650–900 nm)[16] that will promote their biological applications, has grown significantly in recent years.[19–22] Various strategies have been developed to extend the absorption and emission ranges of BODIPYs into the NIR region.[23] Among these approaches, the most widely used one is the Knoevenagel condensation reaction, in which the acidic methyl protons located at the C-3 and C-5 sites of the BODIPY centre react with aromatic aldehydes. Monostyryl BODIPY derivatives are synthesized *via* condensation at the C-3 position, while distyryl BODIPY compounds are obtained by targeting both the C-3 and C-5 regions.[24,25]

Optically inert cores such as cyclotriphosphazenes provide an attractive platform for organizing multiple chromophores in a well-defined manner. Although various multi-BODIPY systems on different inert linkers have been reported, most focus on isolated structures such as dimers or oligomers, rather than a controlled sequence on a single core.[26–29] Conceptually similar triazine-based systems containing 1–2–3 BODIPY units have also been reported,[30] but studies employing a larger number of chromophores on an optically inert central core remain limited. Here, we introduce a controlled model system in which 2, 4, and 6 BODIPY units are attached to the same optically inert cyclotriphosphazene core, enabling a direct and quantitative evaluation of how the number and spatial arrangement of chromophores affect photophysical properties.

Hexachlorocyclotriphosphazene (HCCP), a class of inorganic heterocyclic ring systems, is an important starting agent for the synthesis of substituted molecules that are rele-

[a]*Department of Chemistry, Karabük University, 78050, Karabük, Türkiye. E-mail: semihayildirim@karabuk.edu.tr; Tel: +90 370 4187278*
[b]*Department of Chemistry, Faculty of Science, Gebze Technical University, Gebze, 41400, Kocaeli, Türkiye*

vant for a wide range of applications.[31–36] Six active chlorine atoms in HCCP can be easily functionalized by nucleophilic substitution processes involving various nucleophiles, including amines, organometallic reagents, aryloxides, alkoxides, alcohols, carboxyl groups, *etc*.[37] Cyclotriphosphazenes are widely recognized as being optically inert in the UV-Vis region, with their photophysical properties tunable through the nature of the attached moieties.[38,39] This makes it possible to develop advanced fluorogenic materials suitable for a wide range of applications, while allowing for the controlled adjustment of their photophysical properties.[5,40–42]

Over the past decade, research on BODIPY–cyclophosphazene conjugates has significantly increased.[34,43–47] Herein, to obtain further insight into the photophysical properties on increasing the numbers of BODIPY units onto a cyclotriphosphazene scaffold, we synthesized a systematic series of BODIPY–cyclotriphosphazene conjugates. Hexachlorocyclotriphosphazene allowed for the introduction of different numbers of distyryl-BODIPY units into the structure, thereby enabling control of photophysical properties by varying the amount of distyryl-BODIPY units. The Knoevenagel condensation reaction was used to add alkyl chains to the 3- and 5-methyl sites of the BODIPY core. The structures of the synthesized conjugates were confirmed by MALDI-TOF, ^{1}H NMR, ^{13}C NMR, and ^{31}P NMR analyses. UV–Vis and fluorescence spectroscopic techniques were employed to study the photophysical behaviors of the compounds.

2. Experimental

2.1. Materials

Merck silica gel plates (Kieselgel 60, F_{254} indicator, 0.25 mm) were used for thin-layer chromatography (TLC) and silica gel (Kieselgel 60, 230–400 mesh) for column chromatography. Deuterated solvent ($CDCl_3$) and following chemicals were purchased from Merck; 2,2′-biphenol, trifluoroacetic acid, *p*-chloranil, triethylamine (≥99%), piperidine (≥99%), acetic acid (glacial), dichloromethane, and acetone. Boron trifluoride diethyl etherate (more than 98%) and 1-bromohexane were supplied by Alfa Aesar. 4-Hydroxybenzaldehyde (99%), cesium carbonate and 2,4-dimethylpyrrole (97%) were provided by Acros Organics. Hexachlorocyclotriphosphazene, obtained from Aldrich, was purified by fractional crystallization using *n*-hexane. Potassium carbonate (≥99%), tetrahydrofuran (THF), and benzene were obtained from Sigma-Aldrich. All other chemicals were of the same quality as analytical reagents and were utilised without additional purification unless indicated otherwise.

2.2. Equipment

A Bruker Avance III HD 600 MHz spectrometer was used to record ^{31}P, ^{1}H and ^{13}C NMR spectra at 20 °C in $CDCl_3$ solutions. Mass spectrometry (MS) was performed using the MALDI-TOF technique with a Bruker Daltonics Microflex mass spectrometer. A Shimadzu 2101 UV spectrophotometer was used to record electronic absorption spectra in the UV-visible region. Fluorescence emission spectra were recorded at room temperature using a Varian Eclipse spectrofluorometer. All reactions were monitored by thin layer chromatography using Merck TLC Silica gel plates with a 254 indicator. Silica gel for column chromatography was used for the purifications.

2.3. The parameters for fluorescence quantum yields

The fluorescence quantum yields (Φ_F) of conjugates **6–8** were determined in tetrahydrofuran by comparison with that of zinc(II) phthalocyanine (Φ_{ref} = 0.2/DMSO) as the reference standard.[48] The calculations were carried out using a comparative method (eqn (1)),[45]

$$\Phi_F = \Phi_F(\mathrm{Std})\frac{F \cdot A_{Std} \cdot \eta^2}{F_{Std} \cdot A \cdot {\eta_{Std}}^2} \quad (1)$$

where Φ_F(Std) is the fluorescence quantum yield of the standard. F and F_{Std} are the areas under the fluorescence emission curves of the conjugates (**6–8**) and the standard, respectively. A and A_{Std} are the respective absorbances of the samples and standard at the excitation wavelengths.

2.4. Synthesis

The synthetic pathway used in the preparation of the BODIPY–cyclotriphosphazene conjugates **6–8** is shown in Scheme 1. The aldehyde (**2**),[45] biphenyl substituted cyclotriphosphazenes (**4** and **5**)[39] and BODIPY compounds (**1** and **3**)[45] were synthesized following the procedures described in their respective literature reports.

2.4.1. General synthesis procedure for conjugates 6, 7, and 8. The general procedure for preparing BODIPY-substituted cyclotriphosphazenes (**6–8**) is stated as follows:

The compounds **4**, **5**, and hexachlorocyclotriphosphazene were reacted with distyryl-BODIPY (**3**) using Cs_2CO_3 in dry THF at 25 °C. The progress of the reactions was monitored using silica gel TLC plates with different ratios of dichloromethane : *n*-hexane as the eluent. After the reactions were completed, the cesium chloride (CsCl) formed during the reaction was filtered off, the solvent (THF) was evaporated, and the remaining solids were subjected to column chromatography for purification.

*Synthesis of conjugate **6**.* Compound **3** (93 mg, 0.13 mmol), compound **4** (25 mg, 0.04 mmol) and Cs_2CO_3 (85 mg, 0.26 mmol) were reacted as stated in the general synthesis procedure. Purification of conjugate **6** was achieved through column chromatography, with *n*-hexane/dichloromethane (2 : 1) serving as the eluent (70 mg, 83%).

*Synthesis of conjugate **7**.* Compound **3** (180 mg, 0.25 mmol), compound **5** (23 mg, 0.05 mmol) and Cs_2CO_3 (160 mg, 0.5 mmol) were used. The conjugate **7** was purified *via* column chromatography using *n*-hexane/dichloromethane (3 : 2) as the eluent (96 mg, 60%).

*Synthesis of conjugate **8**.* Conjugate **8** was obtained in a one-step nucleophilic substitution reaction of Cl atoms in hexachlorocyclotriphosphazene with distyryl-BODIPY (**3**) in the presence of cesium carbonate. Compound **3** (100 mg,

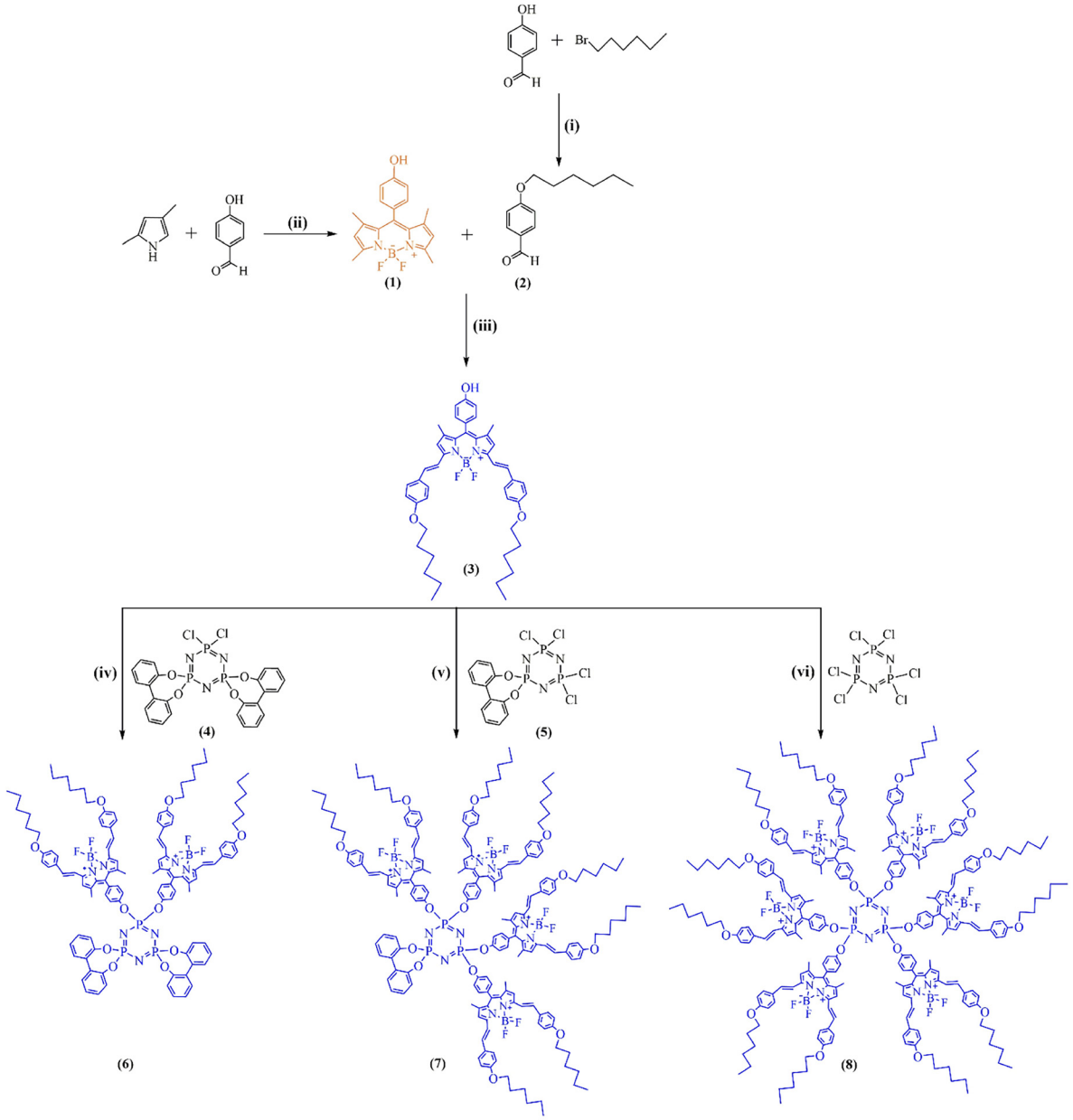

Scheme 1 Structures and synthetic route of BODIPY–cyclotriphosphazene conjugates (**6–8**). (i) K_2CO_3, acetone, 65 °C; (ii) TFA, DCM, DDQ, Et_3N, and BF_3OEt_2; (iii) acetic acid, piperidine, and benzene; and (iv, v, and vi) Cs_2CO_3, THF, 50 °C.

0.14 mmol), hexachlorocyclotriphosphazene (5 mg, 0.014 mmol) and Cs_2CO_3 (114 mg, 0.35 mmol) were used. Column chromatography was performed on conjugate **8** using an *n*-hexane/dichloromethane (1 : 1) mixture as the eluent (46.5 mg, 75%).

3. Results and discussion

3.1. Synthesis and structural characterization

In the present study, compounds **1–5** were initially synthesized following their respective literature procedures.[39,45] Next, the nucleophilic substitution reactions of compounds **4**, **5**, and hexachlorocyclotriphosphazene with the distyryl-BODIPY (**3**) were carried out in molar ratios of 1 : 2, 1 : 4, and 1 : 6, respectively, using Cs_2CO_3 in THF, yielding three new conjugates **6–8**. Scheme 1 presents the synthetic route and structures of the conjugates. All products were purified by column chromatography. Although crystallization was attempted, suitable single crystals for X-ray diffraction analysis could not be obtained. Therefore, the structures of conjugates **6–8** were confirmed by mass spectrometry and detailed ^{31}P, ^{1}H, and ^{13}C NMR spectroscopy.

The MALDI-TOF mass spectra of conjugates **6–8** clearly show the expected molecular ion peaks at *m*/*z* 1934.05,

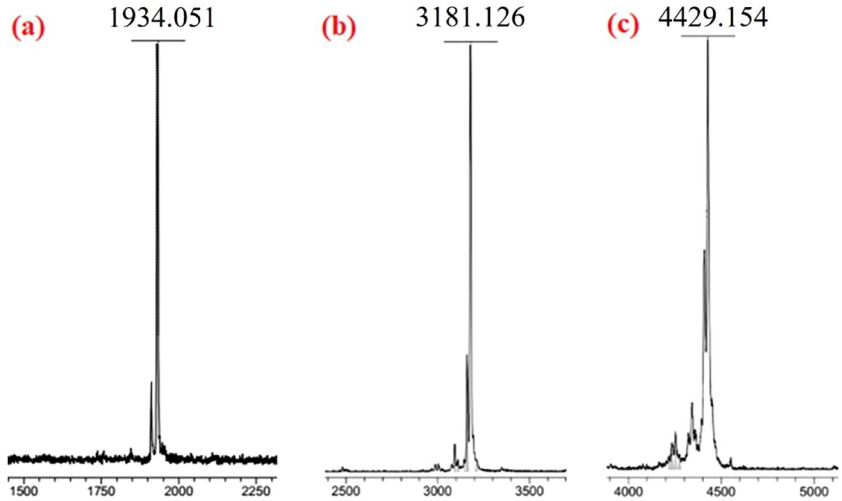

Fig. 1 MALDI TOF-MS spectra of conjugates **6** (a), **7** (b) and **8** (c).

3181.13, and 4429.15, respectively, confirming their successful synthesis (Fig. 1). Full mass spectra for the conjugates are provided in the SI (Fig. S1–S3).

The ^{31}P NMR chemical shifts and $^{2}J_{(PNP)}$ coupling constants of conjugates **6–8** are presented in Table 1. Although multiple substitution patterns are possible, ^{31}P NMR analysis indicates the isolation of a single dominant regioisomer for each derivative, consistent with the literature on cyclotriphosphazene substitution pathways.[49,50] In conjugate **8**, all the phosphorus atoms are equivalent, although conjugates **6** and **7** have two different phosphorus environments within the molecules. Thus, the A_2X and AX_2 spin systems appeared in the ^{31}P NMR spectra of conjugates **6** and **7**, respectively, whereas the A_3 spin system was observed in the spectrum of conjugate **8** (Fig. S4–S6). The signals for spiro P(biph) groups appeared at 25.46 ppm for **6** as a doublet and at 24.62 ppm as a triplet for conjugate **7**, respectively. Similarly, the chemical shifts of the $P(O\text{-}BODIPY)_2$ groups also appeared at 9.84 ppm for **6** and 8.57 ppm for **7**, separately. The ^{31}P NMR spectrum of conjugate **8** exhibited a singlet at 7.35 ppm, consistent with the full substitution of the cyclotriphosphazene core (Table 1).

Generally, the ^{1}H NMR spectra of **6–8** are similar (Fig. 2 and Fig. S7–S9). They all show the distyryl-BODIPY characteristics which were previously presented in the literature.[45] In addition, the signals of aromatic biphenyl groups were also observed in the aromatic range of the spectrum for conjugates **6** and **7**. As an example, the ^{1}H NMR spectrum of conjugate **6** in $CDCl_3$ solution is presented in Fig. 2. Well-resolved ^{1}H NMR data for compound **6** revealed characteristic doublets at 7.20 and 7.60 ppm arising from the *trans*-olefinic protons of the styryl units (*E* configuration, $J \approx 16$ Hz), along with a singlet at 6.60 ppm corresponding to the β-pyrrolic protons. The aromatic protons associated with the biphenyl groups and the aromatic rings of the BODIPY core were observed between 6.90 and 7.57 ppm. The aliphatic $-CH_2$ protons on the distyryl chains of compound **6** resonated in the range of 1.35–3.99 ppm as singlet, triplet, and multiplet signals, while the $-CH_3$ protons on the chains appeared as a triplet at 0.92 ppm. The $-CH_3$ protons on the BODIPY core appeared as a singlet at 1.44 ppm. The integral values and splittings of peaks support the presence and number of biphenyl and BODIPY groups in the structure. Some distinctive peaks in the structure are marked in the spectrum (Fig. 2). The full ^{1}H NMR spectrum for conjugate **6** is provided in the SI (Fig. S7).

The ^{13}C NMR spectral data of the conjugates were also consistent with the molecular structures. The aromatic carbon atoms of the target conjugates **6–8** were observed between 160.1 and 114.8 ppm, while the aliphatic ones were observed between 68.1 and 14.0 ppm in the spectra. It can be seen that the number of peaks in the aromatic region for conjugates **6** and **7** increases with the addition of biphenyl groups to the structure (Fig. S10–S12).

Table 1 ^{31}P NMR parameters of cyclotriphosphazenes in $CDCl_3$ solution

Compound	Spin system	^{31}P NMR (ppm) [P(biph)] (P_A)	^{31}P NMR (ppm) [P(O-BODIPY)] (P_X)	$^{2}J_{(PNP)}$ (Hz) $^{2}J_{AX}$
6	A_2X	25.46	9.84	92.3
7	AX_2	24.62	8.57	94.7
8	A_3	—	7.35	—

3.1.1. Photophysical properties. UV-vis absorption and emission spectroscopywas used to investigate the photophysical properties. All spectroscopic measurements were carried out in a quartz spectroscopic cuvette at room temperature. All measurements were performed in THF at a concentration of 6×10^{-7} M. The normalized absorption spectra of bis-, tetra- and hexa-BODIPY substituted cyclotriphosphazene conjugates (**6–8**) and their precursor BODIPY derivative (**3**) in THF are given in Fig. 3. As shown in Fig. 3a, conjugates **6–8**

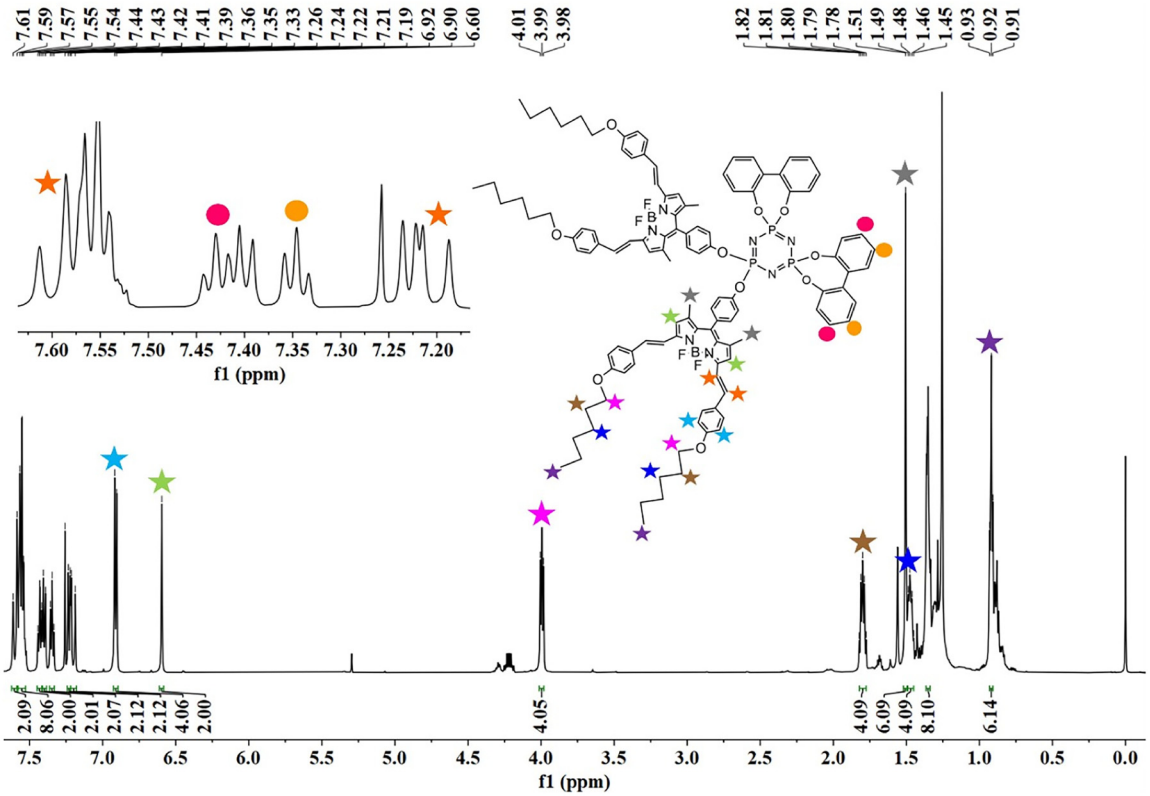

Fig. 2 ^{1}H NMR spectrum of the conjugate **6** in $CDCl_3$ solution.

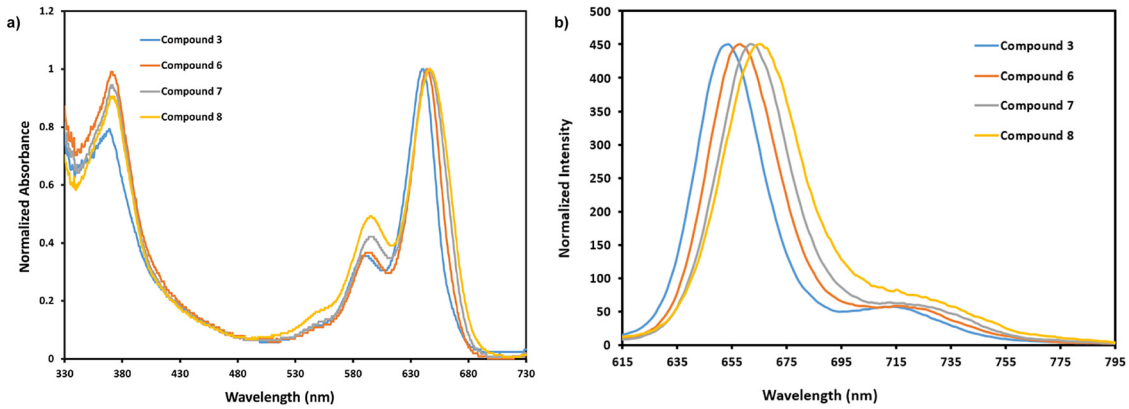

Fig. 3 Normalized absorption (a) and emission (b) spectra of compound **3** and conjugates **6–8** (6×10^{-7} M) in THF.

exhibited UV/Vis absorption behavior similar to that of the BODIPY precursor, as expected.[51] While the unsubstituted cyclotriphosphazene core is completely optically inert in the UV-Vis range,[52] compounds **4** and **5** bearing biphenoxy substituents exhibit characteristic π–π absorption bands in the UV region (*ca.* 240–330 nm). However, their recorded spectra (Fig. S13) clearly show that these transitions do not extend into the visible region. Therefore, although compounds **4** and **5** are not completely optically inert, they are effectively inert in the visible region and do not interfere with the intrinsic $S_0 \rightarrow S_1$ absorption of the BODIPY chromophore.[53] BODIPYs are known to engage in π–π stacking interactions.[54] The strong absorption band of the BODIPY unit, corresponding to the $S_0 \rightarrow S_1$ transitions,[55] was observed at 642 nm for compound **3** and at 645, 646, and 647 nm for BODIPY substituted phosphazene conjugates (**6–8**) with a small red shift, respectively. The small but systematic bathochromic shifts observed in the absorption maxima may be indicative of weak interchromophoric π–π interactions between the closely spaced BODIPY units within the same molecule.[54]

The fluorescence behaviour of the conjugates was observed at a concentration of 6×10^{-7} M in THF. The fluorescence emission maxima were recorded at 654 nm for compound **3**, 658 nm for conjugate **6**, 662 nm for conjugate **7**, and 666 nm for conjugate **8** with a small red shift when excited at 600 nm (Fig. 3b). With the addition of each new distyryl BODIPY unit, the intramolecular π–π interactions increase, leading to a bathochromic shift.[51,56] Connecting several dye units covalently within one molecule creates closely packed fluorophore assemblies that differ in their tendency to undergo intramolecular fluorophore aggregation, a process that substantially modulates their absorption and emission characteristics.[54]

The absorption and emission spectra of the compounds were studied in different solvents (acetone, tetrahydrofuran, methanol, dichloromethane, and DMSO) (Fig. 4 and 5). The spectral shifts observed across the solvent series are very small (only a few nanometers), indicating weak solvatochromic behavior. Although increasing solvent polarity causes minor bathochromic shifts, the almost unchanged shape of the spectral bands—especially the absence of band broadening, additional shoulders, or novel low-energy features—suggests that tightly bound aggregates are unlikely to form under these conditions. Instead, the accompanying decrease in emission intensity may reflect solvent-dependent non-radiative deactivation and interchromophore interaction processes within the densely substituted cyclotriphosphazene structure, while the possible influence of intramolecular self-quenching cannot be ruled out. The three-dimensional cyclotriphosphazene framework, unlike planar cores (*e.g.*, triazine), may partially restrict face-to-face π–π contacts due to the spatial distribution of chromophores; in this case, the decrease in emission intensity, consistent with the absence of band broadening or novel low-energy spectral features in either series, is more reasonably attributable to solvent-dependent non-radiative deactivation pathways and weaker intramolecular interactions rather than well-defined aggregate formation.[57] The lowest emission intensity was observed in the highly polar DMSO for all conjugates. In methanol, a strongly polar protic solvent, both absorption and emission for compounds **6–8** were almost completely quenched, while compound **3** retained strong absorption and emission. This contrasting behavior can be attributed to the significantly higher solubility of compound **3** in methanol and the absence of the large hydrophobic multichromophoric domain found in cyclotriphosphazene-based conjugates (Fig. S14). For derivatives **6–8**, the combination of lower solubility, the apolar nature of the cyclotriphosphazene core, and the broad hydrophobic BODIPY array may promote microaggregation and could enhance nonradiative degradation pathways, potentially resulting in the near-complete loss of optical signals in methanol.

The fluorescence quantum yields (Φ_F) of the conjugates in THF were calculated by comparing with that of the unsubstituted-ZnPc in DMSO solution (Φ_F = 0.2) as the standard for distyryl BODIPY derivatives.[48] The fluorescence quantum

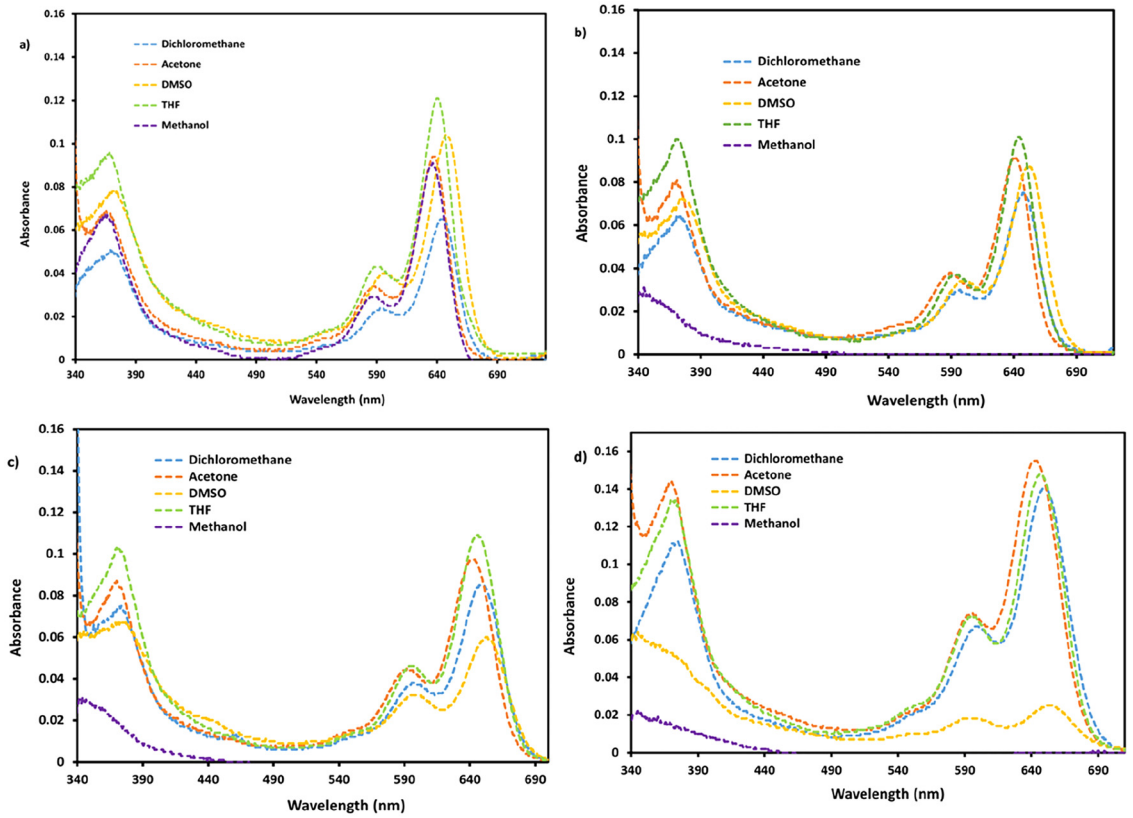

Fig. 4 UV-Vis absorption spectra of (a) compound **3**, (b) conjugate **6**, (c) conjugate **7**, and (d) conjugate **8** (6×10^{-7} M) in various solvents.

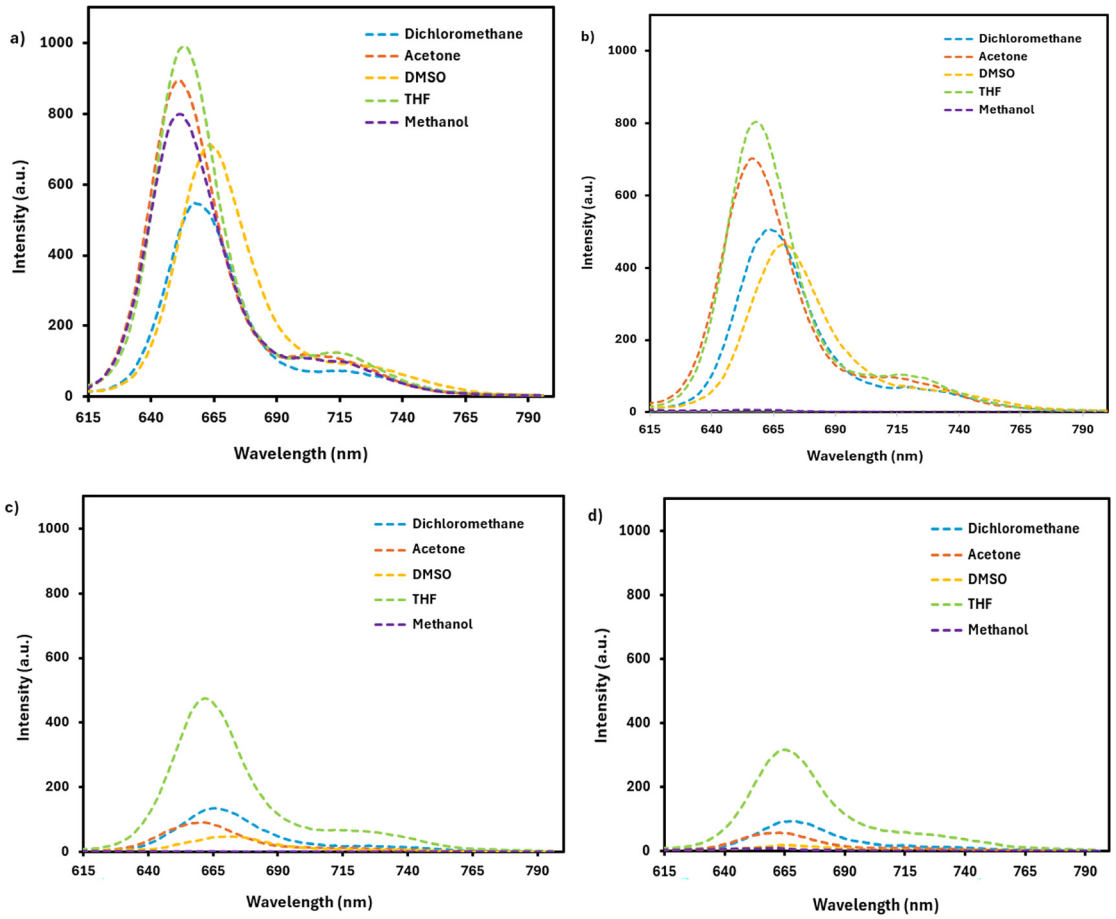

Fig. 5 Fluorescence emission spectra of (a) compound **3**, (b) conjugate **6**, (c) conjugate **7**, and (d) conjugate **8** (6×10^{-7} M) in various solvents (λ_{ex}: 600 nm).

yields were found to be 52%, 49%, 23%, and 11% for compound **3** and conjugates **6–8**, respectively (Table 2). The quantum yields of the conjugates decrease with the increasing number of BODIPY units, as expected.[47,58]

The ground state absorption spectra of the conjugates were also recorded at different concentrations to determine the appropriate concentration for measuring photophysical properties (Fig. S15). The studied concentration ranges were matched with the Lambert–Beer law for the conjugates and 6×10^{-7} M was selected as the working concentration. In addition, the conjugates **6–8** showed good molar extinction coefficients (18 500 M^{-1} cm^{-1}, 24 900 M^{-1} cm^{-1}, and 53 300 M^{-1} cm^{-1}, respectively) in the NIR region of the visible spectrum (Table 2). As the number of BODIPY units attached to the cyclotriphosphazene core increased, the molar absorptivity also increased. This behavior is consistent with previous reports in the literature on multi-BODIPY conjugates.[47,58]

Table 2 Photophysical properties of compound **3** and conjugates **6–8** (6×10^{-7} M) in THF

Compound	λ_{abs} (nm)	λ_{ems} (nm)	ε^a (THF, M^{-1} cm^{-1})	$\Phi_F{}^b$ (%)	Stokes shift, $\Delta\tilde{\nu}^c$ (cm^{-1})
3	369, 642	654	16 950	52	286
6	370, 645	658	18 500	49	306
7	371, 646	662	24 900	23	374
8	372, 647	666	53 300	11	441

[a] Molar extinction coefficients. [b] Fluorescence quantum yield. [c] Stokes shift, $\Delta\tilde{\nu}$ (cm^{-1}) = $10^7/\lambda_{abs} - 10^7/\lambda_{em}$.

4. Conclusion

In conclusion, considering the biological importance of NIR-fluorescence materials, we have attempted to prepare novel BODIPY–cyclotriphosphazenes with different combinations of the same BODIPY group on the cyclotriphosphazene ring. These conjugates exhibited intense absorption bands centered at approximately 646 nm, showing only a slight red shift at low concentration while maintaining high molar extinction coefficients. In contrast, the increasingly red-shifted emission and significantly decreasing quantum yields can be attributed to solvent-dependent non-radiative deactivation and interchromophore interaction processes within the dense spatial arrangement of BODIPY units around the cyclotriphosphazene

core; however, further time-dependent studies will be needed to establish a precise mechanistic picture. We believe that the study presented here provides meaningful insight into molecular structure–property relationships while offering a straightforward and reliable synthetic approach.

Author contributions

Yacinthe Mariole Mache: synthesis, analysis, and investigation. Semiha Yıldırım Sarıkaya: design, methodology, investigation, validation, funding acquisition, project administration, supervision, and writing – original draft. Husniye Ardic Alidagi: formal analysis, investigation, and writing – original draft.

Conflicts of interest

There are no conflicts to declare.

Data availability

The data supporting the findings of this study are available within the article and its supplementary information (SI), which includes NMR spectra, MALDI-TOF data, and additional spectroscopic data. Supplementary information is available. See DOI: https://doi.org/10.1039/d6dt00037a.

Acknowledgements

We are grateful for the financial support from the Scientific Research Unit of Karabük University (Grant No. KBÜBAP-24-YL-132). Open access funding was provided by the Scientific and Technological Research Council of Türkiye (TÜBİTAK).

References

1 Y. Liu, B. Zu and X. Dou, *Coord. Chem. Rev.*, 2025, **532**, 216505.
2 C. S. Mahanta, V. Ravichandiran and S. P. Swain, *ACS Appl. Bio Mater.*, 2023, **6**, 2995–3018.
3 W. Qiao and Z. Li, *Symmetry*, 2022, **14**, 966.
4 A. M. Bongo, J. Shim, S. Cho, J. Lee and H.-J. Kim, *J. Photochem. Photobiol., A*, 2025, **468**, 116469.
5 J. M. Favret and S. V. Dzyuba, *Molecules*, 2025, **30**, 116.
6 M. Zhao, H. Shen and Y. Zhou, *Eur. J. Org. Chem.*, 2024, **27**, e202400701.
7 G.-W. Chen, S.-Y. Li, H.-J. Liu, H. Wang, R. Sun and J.-F. Ge, *Spectrochim. Acta, Part A*, 2025, **329**, 125540.
8 S. Prajapati and S. Jana, *Inorg. Chim. Acta*, 2025, **588**, 122867.
9 V. A. S. Almodovar and A. C. Tomé, *Beilstein J. Org. Chem.*, 2024, **20**, 1933–1939.
10 V. A. S. Almodôvar and A. C. Tomé, *Molecules*, 2021, **26**, 4758.
11 L. Shan, X. Li, Z. Yu, X. Zheng, H. Ren, J. Wu, C. Lv, P. Wang and W. Liu, *Spectrochim. Acta, Part A*, 2025, **343**, 126540.
12 T. Chaivisuthangkura, N. Boosamund, N. Asawutmangkul, T. Khammee, B. Jityuti and W. Siangproh, *Spectrochim. Acta, Part A*, 2025, **327**, 125373.
13 S. Kaleeswaran, D. S. Prabakaran, M. Santhamoorthy, S. Ansar, M. A. Farah, R. Rajamanikandan and K. S. Mani, *Inorg. Chim. Acta*, 2025, **575**, 122440.
14 C. Wu, Y. Yu, J. You, S. Chen, W. Wu and Y. Liang, *Luminescence*, 2025, **40**, e70300.
15 G. Li, J. Du, Z. Wang, C. Ren, F. Lu and Q. Deng, *Dyes Pigm.*, 2024, **222**, 111924.
16 Y. Wang, H. Yu, Y. Zhang, C. Jia and M. Ji, *Dyes Pigm.*, 2021, **190**, 109284.
17 A. Ghosh and A. Adhikary, *J. Mol. Struct.*, 2024, **1317**, 139086.
18 H. Ning, Y. Yang, S. Long, W. Sun, J. Du, J. Fan and X. Peng, *Dyes Pigm.*, 2025, **239**, 112780.
19 Q. Fei, M. Li, J. Chen, B. Shi, G. Xu, C. Zhao and X. Gu, *J. Photochem. Photobiol., A*, 2018, **355**, 305–310.
20 G. Selvaggio, R. Nißler, P. Nietmann, A. Patra, L. J. Patalag, A. Janshoff, D. B. Werz and S. Kruss, *Analyst*, 2022, **147**, 230–237.
21 S. Han, C. Deng, M. Zheng, L. Yang, H. Kong, Y. He, Y. Zheng, G. Deng, Y. Ren and F. An, *Chin. Chem. Lett.*, 2025, **36**, 110459.
22 F. Cheng, T. Qiang, M. Li, B. Wang, K. Liu and K. Li, *Chem. - Eur. J.*, 2025, **31**, e202501427.
23 J. Tao, D. Sun, L. Sun, Z. Li, B. Fu, J. Liu, L. Zhang, S. Wang, Y. Fang and H. Xu, *Dyes Pigm.*, 2019, **168**, 166–174.
24 B. Topaloğlu Aksoy, I. Erol, H. Kandemir, M. F. Saglam, I. F. Sengul and B. Çoşut, *Inorg. Chim. Acta*, 2023, **544**, 121230.
25 S. Zhu, J. Zhang, G. Vegesna, A. Tiwari, F.-T. Luo, M. Zeller, R. Luck, H. Li, S. Green and H. Liu, *RSC Adv.*, 2011, **2**, 404–407.
26 L. J. Patalag, J. Hoche, R. Mitric, D. B. Werz and B. L. Feringa, *Angew. Chem., Int. Ed.*, 2022, **61**, e202116834.
27 A. Patra, L. J. Patalag, P. G. Jones and D. B. Werz, *Angew. Chem., Int. Ed.*, 2021, **60**, 747–752.
28 L. Nayak, S. Acharya, S. Routray, S. Pattnaik and R. Satapathy, *RSC Adv.*, 2025, **15**, 27951–27994.
29 A. S. Sherudillo, L. A. Antina and E. V. Antina, *Coord. Chem. Rev.*, 2025, **545**, 217030.
30 P. Satardekar, V. Chaudhari, Z. A. Siddiqui, S. Lambud, N. Sekar, R. Bhosale and S. More, *New J. Chem.*, 2024, **48**, 17215–17225.
31 J. J. C. Lee, M. H. Chua, S. Wang, Z. Qu, Q. Zhu and J. Xu, *Chem. – Asian J.*, 2024, **19**, e202400357.
32 G. Y. Çiftçi, E. Şenkuytu, M. Bulut and M. Durmuş, *J. Fluoresc.*, 2015, **25**, 1819–1830.
33 A. Uslu and E. Özcan, *Polyhedron*, 2018, **148**, 49–54.
34 E. Şenkuytu and E. Tanrıverdi Eçik, *Spectrochim. Acta, Part A*, 2018, **198**, 232–238.

35 Y. Tümer, *J. Chin. Chem. Soc.*, 2022, **69**, 1897–1907.
36 I. Sharma, R. K. Sinha, S. Shil, S. Rani and N. V. A. Kumar, *ACS Omega*, 2025, **10**, 5312–5323.
37 O. Dagdag and H. Kim, *Polymers*, 2024, **16**, 122.
38 S. O. Tümay, S. Y. Sarıkaya and S. Yeşilot, *J. Lumin.*, 2018, **196**, 126–135.
39 H. İbişoğlu, Ş. Ş. Ün, E. Erdemir and S. O. Tümay, *Phosphorus, Sulfur Silicon Relat. Elem.*, 2021, **196**, 760–768.
40 S. O. Tümay and S. Yeşilot, *J. Photochem. Photobiol., A*, 2019, **372**, 156–167.
41 R. Kagit, M. Yildirim, O. Ozay, S. Yesilot and H. Ozay, *Inorg. Chem.*, 2014, **53**, 2144–2151.
42 D. Palabıyık, C. M. Balcı, S. O. Tümay and S. Beşli, *New J. Chem.*, 2023, **47**, 13866–13879.
43 E. T. Eçik, E. Şenkuytu, Z. Cebesoy and G. Y. Çiftçi, *RSC Adv.*, 2016, **6**, 47600–47606.
44 S. Çetindere, S. O. Tümay, A. Kılıç, M. Durmuş and S. Yeşilot, *Dyes Pigm.*, 2017, **139**, 517–523.
45 S. Y. Sarıkaya, S. Yeşilot, A. Kılıç and E. Okutan, *Dyes Pigm.*, 2019, **162**, 734–740.
46 N. Kwon, K. H. Kim, S. Park, Y. Cho, E.-Y. Park, J. Lim, S. Çetindere, S. O. Tümay, W. J. Kim, X. Li, K. T. Nam, C. Kim, S. Yeşilot and J. Yoon, *Biosens. Bioelectron.*, 2022, **216**, 114612.
47 E. Yıldız Gül, E. Aydin Karataş, H. Aydin Doğan, G. Yenilmez Çiftçi and E. Tanrıverdi Eçik, *Spectrochim. Acta, Part A*, 2024, **311**, 124006.
48 P. Jacques and A. M. Braun, *Helv. Chim. Acta*, 1981, **64**, 1800–1806.
49 S. Beşli, C. Mutlu Balcı, S. Doğan and C. W. Allen, *Inorg. Chem.*, 2018, **57**, 12066–12077.
50 A. Schulz, M. Thormaehlen and H.-C. Müller, *Internet Electron. J. Mol. Des.*, 2003, **2**, 653–677.
51 S. Çetindere, S. O. Tümay, A. Şenocak, A. Kılıç, M. Durmuş, E. Demirbaş and S. Yeşilot, *Inorg. Chim. Acta*, 2019, **494**, 132–140.
52 H. A. Alidağı, S. O. Tümay, A. Şenocak and S. Yeşilot, *Dyes Pigm.*, 2018, **153**, 172–181.
53 E. Özcan, S. O. Tümay, H. A. Alidağı, B. Çoşut and S. Yeşilot, *Dyes Pigm.*, 2016, **132**, 230–236.
54 A. A. Pakhomov, E. E. Kim, Y. N. Kononevich, D. S. Ionov, M. A. Maksimova, V. B. Khalchenia, E. G. Maksimov, A. A. Anisimov, O. I. Shchegolikhina, V. I. Martynov and A. M. Muzafarov, *Dyes Pigm.*, 2022, **203**, 110371.
55 A. A. Pakhomov, A. V. Efremova, M. A. Maksimova, Yu. N. Kononevich, D. S. Ionov, N. O. Dubinets, V. I. Martynov, A. M. Muzafarov and M. V. Alfimov, *High Energy Chem.*, 2023, **57**, 192–199.
56 İ. Ömeroğlu, S. O. Tümay, S. Makhseed, A. Husain and M. Durmuş, *Dalton Trans.*, 2021, **50**, 6437–6443.
57 W. Zhou, H. Guo, J. Lin and F. Yang, *J. Iran. Chem. Soc.*, 2018, **15**, 2559–2566.
58 E. Y. Gül and E. T. Eçik, *ChemPhotoChem*, 2024, **8**, e202300314.